Nuclear quadrupolar spin-lattice relaxation in some III-V compounds*

John A. McNeil†
Department of Physics, University of California, Los Angeles, California 90024 and Fachbereich Physik, Universität Konstanz, 7750 Konstanz, West Germany

W. Gilbert Clark
Department of Physics, University of California, Los Angeles, California 90024
(Received 23 April 1973; revised manuscript received 20 October 1975)

Measurements of the spin-lattice relaxation rates in the group-III-V compounds, GaAs, GaSb, InAs, and InSb, are presented as a function of temperature from 4 to 300 K. These rates, except for GaSb, are separated into magnetic and quadrupolar parts. The quadrupolar rates are separated into relaxation by acoustic phonons and that by optical phonons. A simple phenomenological model fits the data to within 5% over the temperature range. The optical phonons couple more strongly to the III nuclei than to the V. This differential coupling is discussed in terms of a dipole mechanism for the electric field gradients.

I. INTRODUCTION

The first measurements of the nuclear spin-lattice relaxation rates in III-V compounds from 4 to 300 K were made in InSb by Bridges and Clark.[1] The temperature dependence of the data and their simple model showed that the quadrupolar relaxation was sensitive to the gross features of the phonon spectrum for the acoustic modes, and that the optical phonons couple more strongly to the group-III than to the group-V nuclei.

Our object has been to measure and interpret the quadrupolar relaxation throughout the same temperature range in GaAs, GaSb, and InAs, in order to see if the same features noted in the InSb data are common to other III-V compounds. A preliminary report on the subject has been given elsewhere.[2] The four crystals provide an appropriate experimental system, in that each nucleus can be studied in two different but similar environments. However, the data for GaSb could not be fully analyzed because of technical difficulties which are discussed below. It was hoped that the magnitudes, as well as the temperature dependence, of the quadrupolar relaxation rates would become clear. Although the temperature dependence of the rates is found to be characteristic of all these crystals and its common character is now well understood, the systematics of the magnitudes of the rates are still not clear.

A four-parameter phenomenological model is developed and used to interpret the temperature dependence of the data. This model decomposes the quadrupolar relaxation into contributions from the acoustic and optical phonons. By adjusting one parameter for each crystal and two parameters for each nuclear species, this model is within 5% agreement with the data over the entire temperature range 4–300 K. A detailed analysis of the acoustic-phonon contribution is developed from the theory of Bridges[3] and presented in the following paper.[4] Several results from that analysis are relevant to the interpretation of our experimental data. The temperature dependence of the relaxation at low temperatures, regardless of the nature of the spin-lattice coupling mechanism, can be described by a universal function and two adjustable parameters. Also, the TA phonons associated with symmetry points on the Brillouin-zone boundary couple differently to the group-III than to the Group-V nuclear sites, giving rise to the observed fluctuations at low temperatures in the ratio of the relaxation rates of the two nuclear species.

II. EXPERIMENTAL ASPECTS

The samples used in these experiments were prepared from very pure uncompensated single crystals of GaAs and InAs, supplied by Cominco,[5] and of GaSb, supplied by Monsanto.[6] The samples were crushed, sieved to obtain particle sizes in the range 100–200 mesh, and mixed with aluminum powder (size less than 325 mesh) in a ratio of 4:1 by volume. The Al^{27} resonance was used to set the pulse angle and phase of a pulsed NMR spectrometer and to calibrate the equilibrium amplitude of the other resonant nuclei. Teflon capsules contained the powders and provided the form upon which the NMR coil was wound.

All spin-lattice relaxation rates were measured on a pulsed NMR spectrometer of the Clark type,[7] using a single-coil scheme.[8] The regulation of the sample temperature was achieved by a flowing-helium-gas system. With this system the average temperature was known to 0.1% and the regulation

during each run was to within ±0.1%. Five methods of measuring $1/T_1$ were employed, depending upon the magnitude of the spin-lattice relaxation rate and the signal-to-noise ratio at a given temperature. The resulting accuracy of the measured rates over the entire temperature range is about 5%. These methods, as well as details of the experimental apparatus, are discussed elsewhere.[9]

III. EXPERIMENTAL RESULTS

In this section the measurements of the temperature dependence of the total nuclear spin-lattice relaxation rates, $W = 1/T_1$, in GaAs, GaSb, and InAs are presented. The data of Bridges and Clark[1] for InSb are included for completeness and comparison. The total rates are separated into magnetic relaxation and quadrupolar relaxation, and the characteristics of these two contributions are analyzed. Sets of related data are presented on log-log graphs with the same scaling factors to facilitate comparison. The major features of these measurements are identified and numbered so that they can be referred to easily later in the discussion. Interpretation of the data will be the subject of Sec. IV.

A. Total relaxation rates

The total spin-lattice relaxation rates W in GaAs, GaSb, and InAs measured in this study are presented in Figs. 1–3. The data of Bridges and Clark[1] for InSb are shown in Fig. 4. Features pertinent to each figure are noted in the caption or on the graph. The following characteristics appear in common:

(i) At the lowest temperatures, the relaxation exhibits a weak temperature dependence. As we shall see later the quadrupolar relaxation which dominates at higher temperatures is strongly temperature dependent and is orders of magnitude smaller than observed in this temperature regime. This weakly temperature-dependent rate will be identified as magnetic relaxation W_M.

(ii) The magnetic relaxation W_M of each species in three of the samples remains parallel, i.e., exhibits the same temperature dependence. This is not true for GaSb (Fig. 2).

(iii) There is a rapid increase in rate with temperature owing to the quadrupolar relaxation rate W_Q becoming comparable in magnitude with the magnetic relaxation rate W_M.

(iv) In the temperature regime where $W_Q \gg W_M$, the relaxation of the isotopes has the same temperature dependence (the curves are parallel). This is not true for nuclei of different atomic species.

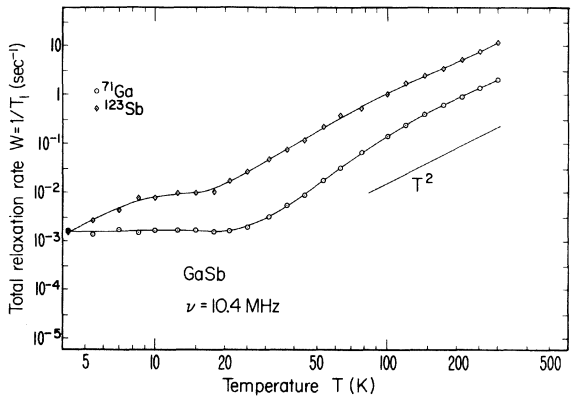

FIG. 2. Measured total nuclear spin-lattice relaxation rates of ^{71}Ga and ^{123}Sb in GaSb as a function of temperature. The solid lines are smoothed interpolations for the data points.

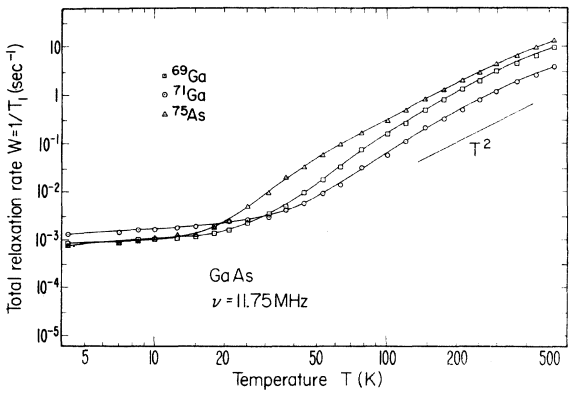

FIG. 1. Measured total nuclear spin-lattice relaxation rates of ^{69}Ga, ^{71}Ga, and ^{75}As in GaAs as a function of temperature. The solid lines are smooth interpolations for the data points.

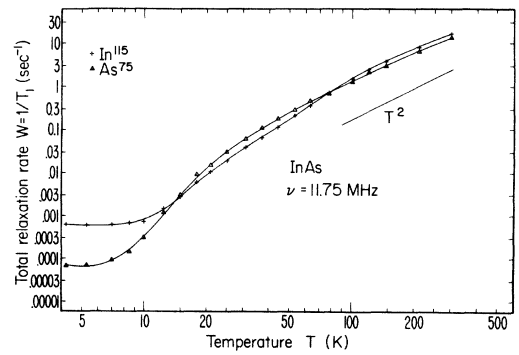

FIG. 3. Measured total nuclear spin-lattice relaxation rates of ^{115}In and ^{75}As as a function of temperature. The solid lines are smooth interpolations for the data points.

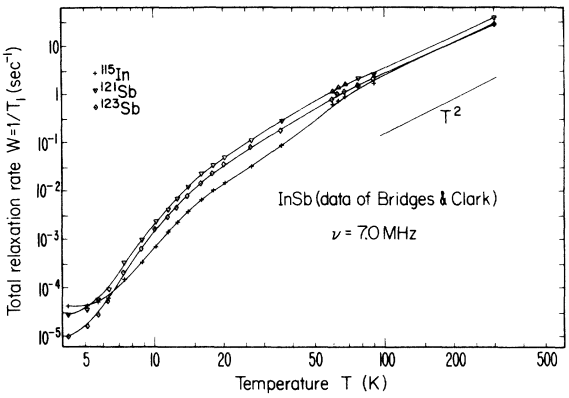

FIG. 4. Measured total nuclear spin-lattice relaxation rates of ^{115}In, ^{121}Sb, and ^{123}Sb in InSb. The data are from Bridges and Clark, Ref. 1. The solid lines are smooth interpolations for the data points.

(v) At the highest temperatures, all rates become proportional to the square of the temperature.

B. Separation of magnetic and quadrupolar relaxation rates

Since the primary interest of this study lies in the quadrupolar relaxation, it is necessary to subtract out the magnetic relaxation. Observations (ii) and (iv) permit the use of a method similar to that of Warren and Clark[10] to separate the competing rates for isotopes in a given crystal. Three of our crystals have isotopes: GaAs (^{69}Ga and ^{71}Ga), InSb (^{121}Sb and ^{123}Sb), and GaSb. However, the method cannot be applied to GaSb, since at 10.4 MHz the ^{69}Ga and ^{121}Sb resonances are only 29 G apart, and experimentally it is difficult to measure their individual relaxation rates. Therefore no separation was attempted in GaSb.

The total rates of the two isotopes (A and B) are to be separated into magnetic and quadrupolar parts:

$$W^A = W_M^A + W_Q^A , \tag{1a}$$

$$W^B = W_M^B + W_Q^B , \tag{1b}$$

It is well known from theory[11] that the quadrupolar rate for the zinc-blende structure is isotropic and depends on the nuclear coordinates in the following manner:

$$W_Q = f(I) Q^2 S(T) , \tag{2}$$

where

$$f(I) = (2I+3)/I^2(2I-1) , \tag{3}$$

and I and Q are the spin and quadrupole moment of the nucleus, respectively. The function $S(T)$ depends only upon the environment and is related to the square of the local electric field gradient. In this paper it is referred to as the "relaxation function." Since it is independent of the nuclear coordinates, it has the same value for isotopes. Therefore the ratio of the quadrupolar rates is temperature independent,

$$R_Q = \frac{W_Q^B}{W_Q^A} = \frac{f(I_B)\, Q_B^2}{f(I_A)\, Q_A^2} . \tag{4}$$

The ratio of the quadrupole moments of isotopes is known with precision from nuclear-quadrupole-resonance experiments.[12] For gallium, we calculate

$$R_Q = W_Q^{69}/W_Q^{71} = 2.517\,620 , \tag{5}$$

and for antimony,

$$R_Q = W_Q^{123}/W_Q^{121} = 0.690\,900 . \tag{6}$$

This provides a qualitative explanation for observation (iv). As a quantitative check, the ratio of the total relaxation rates for the gallium isotopes in GaAs was averaged from 77 to 600 K and found to be

$$R_Q = 2.50 \pm 0.05 . \tag{7}$$

For this reason the relaxation in this temperature regime is seen to be entirely quadrupolar.

The magnetic relaxation is due to spin diffusion to paramagnetic impurities, and the dependence of this relaxation on the nuclear coordinates is unknown from theory. Observation (ii), however, suggests that we can assume that the ratio of the magnetic rates is a constant which can be determined by the ratio of total rates at low temperatures, where the quadrupolar rate is small. Thus we define

$$R_M = W_M^B/W_M^A . \tag{8}$$

Equations (1), (3), and (8) can be solved for each component:

$$W_M^A = (W^B - R_Q W^A)/(R_M - R_Q) , \tag{9a}$$

$$W_Q^A = W^A - W_M^A , \tag{9b}$$

$$W_M^B = R_M W_M^A , \tag{9c}$$

$$W_Q^B = R_Q W_Q^A . \tag{9d}$$

It should be noted that the entire temperature dependence of the background relaxation W_M is determined to within a multiplicative constant by the measured rates of W^A and W^B and the precisely known value of R_Q, and is independent of the value R_M. (This is fortunate, since the value of R_M in InSb is uncertain because of the large amount of quadrupolar relaxation that remains even at the lowest temperature.)

For the nuclei in each crystal which are not isotopes, observation (ii) suggests that the magnetic components are proportional. The proportionality constant R_M has been fixed at the low-

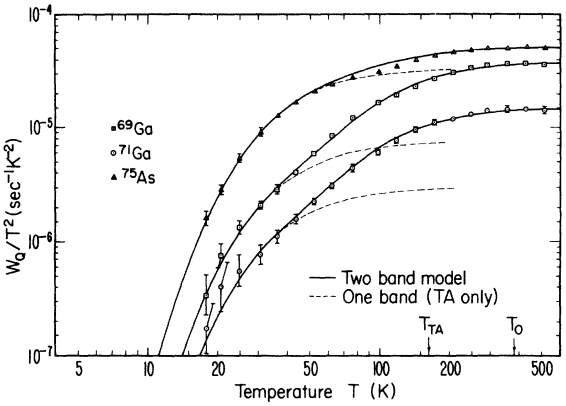

FIG. 5. Measured quadrupolar relaxation function W_Q/T^2 for ^{69}Ga, ^{71}Ga, and ^{75}As in GaAs as a function of temperature. Note the increased rate of the group-III nuclei (^{69}Ga, ^{71}Ga) relative to the group-V nuclei (^{75}As) at T_{TA}.

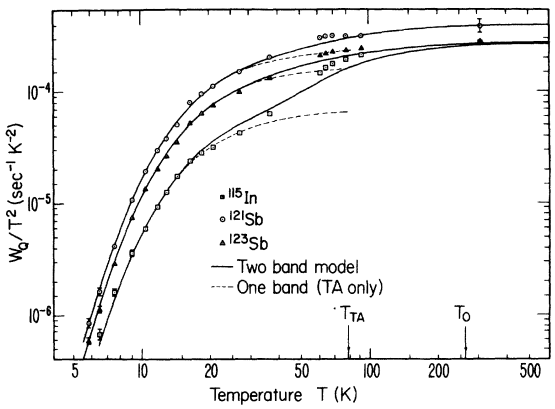

FIG. 7. Measured quadrupolar relaxation function W_Q/T^2 of ^{115}In and ^{123}Sb in InSb as a function of temperature. Note the increased rate of the group-III nucleus (^{115}In) relative to the group-V nucleus (^{121}Sb, ^{123}Sb) at T_{TA}. The data are from Ref. 1.

temperature end. An interpretation of the origin of W_M is given in Ref. 9.

C. Quadrupolar relaxation

With the magnetic relaxation separated out, we can examine the temperature dependence of the quadrupolar relaxation. Both theory[13] and observation (iv) indicate that, at high enough temperatures, W_Q is quadratic in temperature. It is convenient and instructive to divide out this temperature behavior and consider the quantity W_Q/T^2. Figures 5–7 show the temperature dependence of W_Q/T^2 in GaAs, InAs, and InSb. Whereas W_Q varies over seven orders of magnitude, W_Q/T^2 varies only over three. Observations (iv) and (v) are clearly accentuated. In addition to these, we add the following:

(vi) At low temperatures the rates of the group-III and group-V nuclei remain relatively parallel. However, in the middle temperature range there is a larger fractional increase in the rate as a function of temperature for the group-III nuclei than for the group-V nuclei.

This differential relaxation of the group-III and group-V nuclei is surprising when one considers that the same phonons, which are being thermally excited at a given temperature, are relaxing both types of nuclei. We can divide out the nuclear coordinates and look at the temperature dependence of the relaxation function, $S(T)$, as defined in Eq. (2). A logarithmic plot of $S(T)$ would yield curves identical to those of W_Q, only shifted vertically, with those of isotopes on top of each other. It is interesting to look at the change in the distance

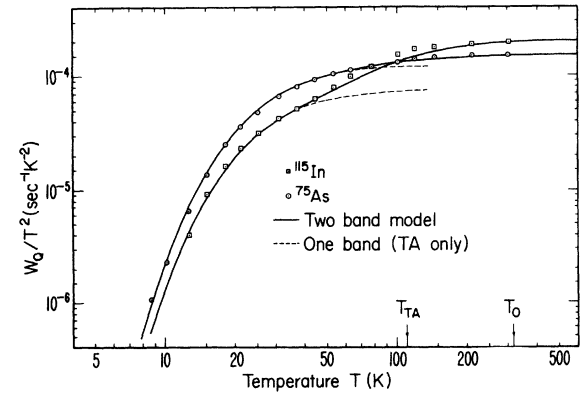

FIG. 6. Measured quadrupolar relaxation function W_Q/T^2 for ^{115}In and ^{75}As as a function of temperature. Note the increased rate of the group-III nucleus (^{115}In) relative to the group-V nucleus (^{75}As) at T_{TA}.

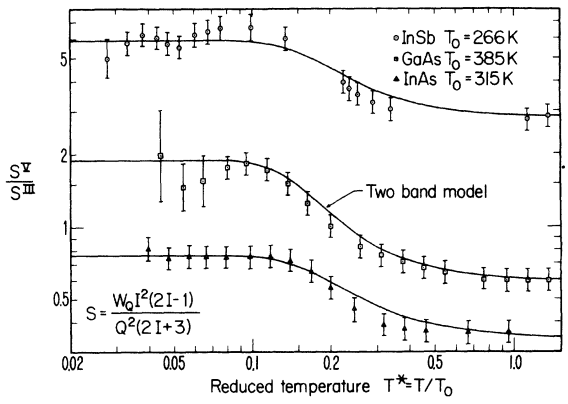

FIG. 8. Ratio of the local relaxation function at the group-III and group-V nuclear sites as a function of temperature. The value of T_0 corresponds to the temperature of the TO (Γ) phonons. This figure shows the relative change in the local field as optical phonons are thermally excited.

between the group-III and group-V curves, i.e., the temperature dependence of the ratio of the local fields. A plot of S^{V}/S^{III} versus temperature is shown in Fig. 8. (The temperature on this graph has been reduced by a value T_0, which is chosen to correspond to the frequency of the transverse-optical phonons, for reasons to be given in Sec. IV). The enhancement in the relaxation function at the group-III site is evident from the drop in the ratio at temperatures about $0.2T_0$. From this graph are drawn the following observations:

(vii) The ratio in all cases drops with an increase in temperature. The change in the ratio for the two indium compounds is the same, a factor of 2.10, while that in GaAs is larger, a factor of 3.15.

(viii) At the lowest temperatures, the relaxation function $S(T)$ is largest at the site with the largest atomic number. The atomic numbers of Ga, As, In, and Sb are 31, 33, 49, and 51. At low temperatures the ratio is greater than unity for InSb and GaAs, and less than unity for InAs.

(ix) In the GaAs and the InSb samples, the ratio of the local relaxation functions at low temperatures is not constant, but in fact has a small fluctuating temperature dependence. This fluctuation is discussed in the following paper.[4]

IV. INTERPRETATION

In this section the experimental quadrupolar relaxation rate data are analyzed. First, the general theory of quadrupolar relaxation is outlined to provide a basis for a phenomenological model, which is then discussed. When applied to the data, this "two-band model" is found to describe the relaxation rates to within experimental error (5%) over the entire temperature range. The model indicates that the relaxation by the optical phonons is stronger for the group-III nuclei than for the group-V nuclei. An explanation for this differential coupling is presented.

A. General theory of quadrupolar relaxation

Quadrupolar relaxation results from magnetic transitions induced by the coupling of the nuclear quadrupolar moment to the electric field gradients at the nuclear site. The term in the Hamiltonian expressing this coupling is of the form

$$H_Q = \sum_{\mu=-2}^{2} A_{-\mu} V_\mu \,, \tag{10}$$

where A_μ and V_μ are the spherical components of nuclear quadrupole moment and the electric field gradients, respectively. The exact form of each component is noted elsewhere.[14] Mieher has shown[11] that if a spin temperature exists, the nuclear quadrupolar relaxation rate is

$$W_Q = Df(I) \sum_{\mu=-2}^{2} \mu^2 W^\mu \,, \tag{11}$$

where $f(I)$ is given in Eq. (3),

$$D = \tfrac{1}{40} e^2 Q^2 \,, \tag{12}$$

and

$$W^\mu = \frac{2\pi}{\hbar} \sum_{nn'} |\langle n' | V_\mu | n \rangle|^2 \delta(E_{n'} - E_n - \mu\hbar\omega_0) \,. \tag{13}$$

The gradients V_μ are produced by the dynamic displacement from equilibrium position of the surrounding charges caused by phonons. The functions $|n\rangle$ denote the states of the lattice vibrations. The spin-temperature approximation is appropriate for these III-V compounds, since the spin-spin relaxation time T_2, which is on the order of 10^{-4} sec, is much shorter than the spin-lattice relaxation time. The important thing to note here is that the dependence of the relaxation upon the nuclear spin coordinates is completely determined, even though nothing has been assumed regarding the electric field gradients. This result was used in Sec. III.

Conservation of energy, as expressed by the δ function, and Bose-Einstein statistics restrict the possible types of mechanisms which can be effective for relaxation to Raman processes,[11] i.e., one phonon is absorbed and one is emitted with an energy increase equal to the loss of nuclear Zeeman energy. Two types of Raman processes have been proposed.[13] The first is the "harmonic Raman process," in which two phonons are coupled directly with the nucleus. The other is the "anharmonic Raman process," which is a second-order interaction wherein a single virtual phonon is coupled to the nucleus by a direct process and to two other phonons by the anharmonic part of the crystal potential. In either case, Eq. (11) can be written in the form

$$W_Q = \frac{e^2Q^2}{40} \frac{f(I)}{\hbar^4} \frac{4\pi}{M^2} \times \sum_{\vec{\lambda},\vec{\lambda}'} n_{\vec{\lambda}}(n_{\vec{\lambda}'}+1) \frac{H(\vec{\lambda},\vec{\lambda}')}{\omega_{\vec{\lambda}}^2} \delta(\omega_{\vec{\lambda}} - \omega_{\vec{\lambda}'}) \tag{14}$$

where the two phonons are identified by the indices $\vec{\lambda} = \vec{k}, p$ and $\vec{\lambda}' = \vec{k}', p'$; $\vec{k}$ and $\vec{k}'$ are their respective wave vectors, and p and p' are their polarizations. $\omega_{\vec{\lambda}}$ is the angular frequency of the phonon and $n_{\vec{\lambda}}$ is its thermal equilibrium population given by the Bose-Einstein factor

$$n_{\vec{\lambda}} = 1/(e^{\hbar\omega_{\vec{\lambda}}/kT} - 1) \,. \tag{15}$$

The mass of the crystal is M. Since the nuclear

Zeeman energy is 10^{-5} smaller than the phonon energies, it has been dropped from the δ function. There is very little, if any, overlap in energy between the acoustical and optical branches in the III-V compounds. Therefore the δ function restricts λ and λ' to the same branch, but not necessarily to the same polarization or wave vector. All of the details of the coupling of the two phonons are contained in the coupling term $H(\vec{\lambda}, \vec{\lambda}')$. The entire temperature dependence stems from the factors $n_{\vec{\lambda}}(n_{\vec{\lambda}}+1)$, which can be expressed as

$$n_{\vec{\lambda}}(n_{\vec{\lambda}}+1) = \left|kT/\hbar\omega_{\vec{\lambda}}\right|^2 E^*(kT/\hbar\omega_{\vec{\lambda}}) \ , \tag{16}$$

where

$$E^*(x) = \left|2x\sinh(1/2x)\right|^{-2} \ . \tag{17}$$

This function $E^*(x)$ has the important property that it approaches unity as its argument becomes arbitrarily large. It will be called the optical function. Equation (14) becomes

$$\frac{W_Q}{T^2} = C\sum_{\vec{\lambda},\vec{\lambda}'} \frac{H(\vec{\lambda},\vec{\lambda}')}{\omega_{\vec{\lambda}}^4} E^*\left(\frac{kT}{\hbar\omega}\right)\delta(\omega_{\vec{\lambda}} - \omega_{\vec{\lambda}'}) \ , \tag{18}$$

where

$$C = \tfrac{4}{40}\pi f(I)\left|eQk/M\hbar^3\right|^2 \ . \tag{19}$$

For temperatures sufficiently greater than any $\omega_{\vec{\lambda}}$, the quantity W_Q/T^2 becomes independent of temperature because of the limiting behavior of E^*,

$$\frac{W_Q}{T^2} = C\sum_{\vec{\lambda},\vec{\lambda}'} \frac{H(\vec{\lambda},\vec{\lambda}')}{\omega_{\vec{\lambda}}^4}\,\delta(\omega_{\vec{\lambda}} - \omega_{\vec{\lambda}'}) \ . \tag{20}$$

Thus the high-temperature $W_Q \propto T^2$ behavior arises strictly from the two-phonon statistics and is not dependent upon the details of the mechanism or approximations. Experimentally this behavior is seen in Figs. 1–7, and was noted in observation (v) in Sec. III.

The term $H(\vec{\lambda}, \vec{\lambda}')$ is

$$H(\vec{\lambda},\vec{\lambda}') = \left|f(\vec{\lambda},\vec{\lambda}') + g(\vec{\lambda},\vec{\lambda}')\right|^2 \ , \tag{21}$$

where $f(\vec{\lambda}, \vec{\lambda}')$ expresses the harmonic Raman process and $g(\vec{\lambda}, \vec{\lambda}')$ the anharmonic Raman process; the exact forms for these functions are given in Ref. 13. In principle these terms must be calculated for each pair of points in the Brillouin zone. Only approximate calculations have been attempted.[1,2,11,13]

B. Two-band phenomenological model

Now we turn to the following approximate evaluation of Eq. (18), which is a development of the theories of Bridges and Clark[1] and Bridges.[2] The restricted double summation becomes a single integration over frequency and a summation over polarizations if the dispersion curve for each phonon branch is assumed to be isotropic. Although the measured dispersion curves in[15] InSb and[16] GaAs show that this is not the case, effects associated with the anisotropy are expected to be averaged out due to the summation over all pairs of phonons on each frequency surface. (It is shown in the following paper[4] that this averaging is not complete.) On the assumption of isotropic dispersion curves, Eq. (18) becomes

$$\frac{W_Q}{T^2} = C\sum_{pp'}\int \rho_p(\omega)\rho_{p'}(\omega)\frac{H_{pp'}(\omega)}{\omega^4}E^*\left(\frac{kT}{\hbar\omega}\right)d\omega \ , \tag{22}$$

where $H_{pp'}(\omega) = \langle H(\vec{\lambda}, \vec{\lambda}')\rangle$, the symbol $\langle\cdots\rangle$ indicating the average over all directions for pairs of phonons with polarization p and p' and frequency ω, and where $\rho_p(\omega)$ is the density of phonon states.

The phonon density of states is available from the calculation for diamond-type lattices by Phillips.[17] His results for germanium are shown in Fig. 9. The distributions are functionally similar for Ge, Si, Sn, InSb, and GaAs, although the frequencies for each branch of the distribution scale differently. From Fig. 9 it is seen that one-third of the phonon states lie in the transverse-acoustic (TA) modes, which would be the only modes thermally excited at low temperatures. It is also seen that one-third of the phonon states lie in a narrow band at the optical frequencies. They are important for relaxation at high temperatures.

To evaluate Eq. (22) the density of states from Fig. 9 is used. Because there is no overlap between the acoustic and optical density of states, the summation over the polarizations splits into two parts. The spike in the density of states of

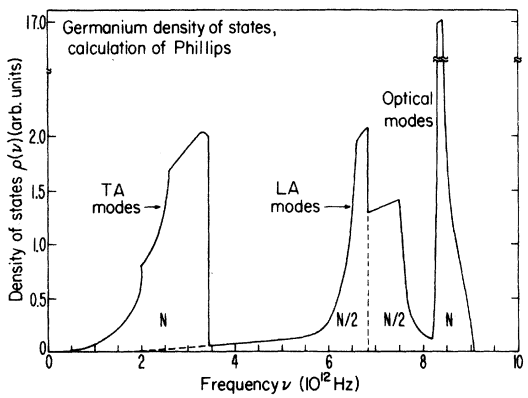

FIG. 9. Phonon density of states in germanium. This frequency distribution was calculated from measured dispersion curves by Phillips, Ref. 17.

TABLE I. Acoustic function $E_A(T^*)$ vs T^*.

T^*	$E_A(T^*)$	T^*	$E_A(T^*)$
0.0200	1.452×10^{-6}	0.258	0.467
0.0222	2.31×10^{-6}	0.286	0.531
0.0245	3.69×10^{-6}	0.316	0.591
0.0272	6.00×10^{-6}	0.350	0.647
0.0301	1.001×10^{-5}	0.388	0.697
0.0333	1.740×10^{-5}	0.430	0.742
0.0369	3.22×10^{-5}	0.476	0.782
0.0409	6.44×10^{-5}	0.527	0.817
0.0453	1.374×10^{-4}	0.584	0.847
0.0502	3.05×10^{-4}	0.647	0.872
0.0556	6.80×10^{-4}	0.717	0.894
0.0616	1.479×10^{-3}	0.794	0.912
0.0682	3.09×10^{-3}	0.879	0.928
0.0756	6.13×10^{-3}	0.974	0.940
0.0837	1.150×10^{-2}	1.079	0.951
0.0927	2.04×10^{-2}	1.195	0.960
0.1027	3.42×10^{-2}	1.324	0.967
0.1138	5.44×10^{-2}	1.466	0.973
0.1260	8.21×10^{-2}	1.624	0.978
0.1396	0.1183	1.799	0.982
0.1546	0.1628	1.993	0.985
0.1713	0.215	2.21	0.988
0.1897	0.274	2.45	0.990
0.210	0.337	2.71	0.992
0.233	0.402	3.00	0.993

the optical modes has the effect of a δ function at the angular frequency ω_0 of the transverse-optical (TO) (Γ) phonons. Thus Eq. (22) becomes

$$\frac{W_Q}{T^2} = \left|\frac{W_Q}{T^2}\right|_{ac} + \left|\frac{W_Q}{T^2}\right|_{op} , \tag{23}$$

with

$$\left|\frac{W_Q}{T^2}\right|_{ac} = C \sum_{pp'}{}' \rho_p(\omega)\rho_{p'}(\omega) \frac{H_{pp'}(\omega)}{\omega^4} E^*\left(\frac{kT}{\hbar\omega}\right) d\omega \tag{24}$$

and

$$\left|W_Q/T^2\right|_{op} = BE^*(kT/\hbar\omega_0) , \tag{25}$$

where B will be treated as an adjustable parameter. The summation in Eq. (24) is restricted to the acoustic modes.

Bridges has calculated the acoustic relaxation contribution Eq. (24) for a general interaction involving only nearest neighbors. His calculation included only the transverse and longitudinal phonons with frequencies up to the maximum TA phonon frequencies. The calculation is extended in the following paper[4] to include all of the acoustic phonons, and is generalized for an arbitrary mechanism for the coupling of the nearest neighbors to the nuclear quadrupole moment. It is shown that over the temperature range of interest the resulting temperature dependence of the relaxation due to the acoustic phonons is of the form

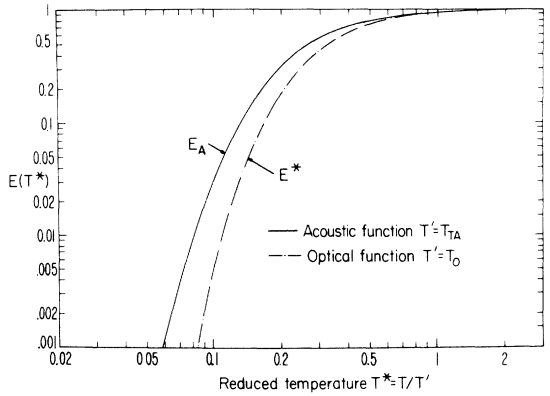

FIG. 10. Relaxation functions as a function of reduced temperature. The acoustic function for relaxation by the acoustic phonons is based upon the realistic density of states calculated by Phillips, Ref. 17. The optical function for relaxation by the optical phonons is based upon an Einstein density of states at the TO (Γ) frequency.

$$\left|W_Q/T^2\right|_{ac} = AE_A(kT/\eta\hbar\omega_{TA}) , \tag{26}$$

where A is a scaling factor for the amplitude of the relaxation, calculable in principle, but an adjustable parameter in practice. The function $E_A(T^*)$ is called the acoustic function and is listed in Table I. The temperature scaling parameter η is a number on the order of 1 and depends upon the nature of the coupling of the nearest neighbors to the nuclear quadrupole. (It equals 1 for the special case of a harmonic Raman process and a point-charge mechanism for the electric field gradients.) Since the details of the coupling mechanism are not known, $\eta\omega_{TA}$ is considered an adjustable parameter to be determined by the data. By redefining parameters,

$$T_{TA} = \hbar\omega_{TA}/k , \tag{27a}$$

$$T_0 = \hbar\omega_0/k , \tag{27b}$$

the total relaxation becomes

$$W_Q/T_2 = AE_A(T/T_{TA}) + BE^*(T/T_0) . \tag{28}$$

The acoustic and optical functions are shown in Fig. 10.

Now consider the application of this two-band model to the experimental data for GaAs, InAs, and InSb. The parameters A, B, and T_{TA} in Eq. (28) were best fitted in the least-squares sense to the data. The value of T_0 was calculated from restrahlen spectra.[18] The resultant two-band-model fit to the data is shown in Figs. 5–7. The broken curve shows the relaxation due to the acoustic phonons alone. The deviation of the solid curve from the broken curve is due to the optical phonons. It can be seen that the two-band mod-

TABLE II. Best-fit parameters.

Species	$W_Q/T^2 = AE_A(T/T_{TA}) + BE^*(T/T_0)$ A (10^{-5} sec^{-1} K^{-2})	T_{TA} [b] (K)	$\eta\omega_{TA}$ ($2\pi\times10^{12}$ Hz)	B (10^{-5} sec^{-1} K^{-2})	T_0 [b] (K)	ω_0 [a] ($2\pi\times10^{12}$ Hz)
^{69}GaAs	0.783 ±0.045			2.97 ±0.20		
^{71}GaAs	0.310 ±0.015	165.8 ±0.6	3.46 ±0.01	1.18 ±0.65	385	8.02 [c]
Ga^{75}As	3.43 ±0.03			1.71 ±0.10		
^{115}InAs	7.84 ±0.40	111 ±1	2.32 ±0.02	12.6 ±1.0	315	6.57 [d]
In^{75}As	12.95 ±0.40			2.1 ±0.3		
^{115}InSb	8.37 ±0.35			18.6 ±1.3		
In^{121}Sb	25.8 ±0.7	83.0 ±0.6	1.73 ±0.01	13.7 ±2.0	266	5.54 [e]
In^{123}Sb	17.8 ±0.8			9.5 ±1.4		

[a] Frequency of TO (Γ) phonons was not fitted to the data, but was taken from published values.
[b] $T_0 = \hbar\omega_0/k$; $T_{TA} = \eta\hbar\omega_{TA}/k$.
[c] See Ref. 16.
[d] See Ref. 18.
[e] See Ref. 15.

el fits the data to within 5% over the entire temperature range. The values of the fit parameters are listed in Table II.

The best-fit values of the parameter $\eta\omega_{TA}$ are 3.46 ± 0.01 and 1.73 ± 0.01 ($2\pi\times10^{12}$ Hz) for GaAs and InSb, respectively. Neutron diffraction measurements of the dispersion curves of[16] GaAs and[15] InSb give ω_{TA} as 3.48 ± 0.06 and 1.82 ± 0.02 ($2\pi\times10^{12}$ Hz), respectively. This implies that the factor η is 0.99 ± 0.02 and 0.95 ± 0.01 for these two crystals, which is within the expected range for this parameter.[4]

The two-band model provides a phenomenological expression for the ratio of the relaxation functions at the group-III and group-V nuclear sites as a function of temperature, shown as the solid line through the data points in Fig. 8,

$$\frac{S_V}{S_{III}} = \left(\frac{f(I_{III})Q_{III}^2}{f(I_V)Q_V^2}\right)\frac{A_V E_A(T/T_{TA}) + B_V E^*(T/T_0)}{A_{III}E_A(T/T_{TA}) + B_{III}E^*(T/T_0)} . \tag{29}$$

According to this model the ratio remains constant for temperatures below $0.1T_0$. Figure 8 and observation (ix), however, show that this ratio fluctuates. What is being seen are small deviations from the Bridges theory due to approximations. This model and these fluctuations are examined in greater detail in the following paper.[4] Here we simply point out that some terms which have been left out of the Bridges theory make a small contribution to the relaxation and are difficult to calculate. Their omission removes all temperature dependence to the ratio of relaxation rates from acoustic phonons. However, even if these terms are included, the use of an isotropic model for the dispersion curves permits only a monotonic temperature dependence, rather than the fluctuating one seen in the data. They are attributed to the differential coupling of particular phonons in the vicinity of symmetry points on the Brillouin-zone boundary to the two nuclear sites.

C. Dipole mechanism for relaxation by optical phonons

It is clear from Figs. 5–7 that the optical phonons couple more strongly to the group-III nuclei than to the group-V nuclei. This differential coupling of the optical phonons (relative to the acoustic phonons) is also seen in Fig. 8, where the ratio of the local relaxation function at the group-III and group-V nuclear sites decreases for $T > 0.15T_0$, the range in which the relaxation by optical phonons becomes important. This can be seen quantitatively from the best-fit parameters in Table II. The ratio of the amplitudes of the optical and the acoustic phonons, B/A, for the group-III nuclei is 3.80, 1.60, and 2.22 for GaAs, InAs, and InSb, respectively, while the ratio for the group-V nuclei is only 0.50, 0.16, and 0.53. It has been suggested previously that a dipole mechanism, such as has been proposed by Wikner *et al.*[19] and generalized somewhat by Joshi *et al.*,[20] could account for this differential coupling. In this mechanism the phonons induce an electric field at the atomic sites. Depending upon the polarizabilities of the atoms, a time-varying dipole moment is induced which contributes to the electric field gradients at the neighboring sites. It is known from optical data[21] on the group-III-V compounds that the polarizabilities of the group-V atoms are greater than those of group III. Therefore we would expect that, insofar as this mechanism contributes to the relaxation, the group-III nuclei would be relaxed more rapidly than the group-V nuclei.

This dipole mechanism should contribute to the relaxation by the acoustic phonons as well as the optical. However, the density of states for the optical phonons peaks strongly for phonons at the center of the Brillouin zone, as can be seen in Fig. 9, and these phonons produce intense electric fields. Therefore the dipole mechanism is much more effective for the optical phonons than for the acoustic. For this reason we would expect the differential coupling to the group-III and group-V nuclei of this mechanism to be important at temperatures where the optical phonons are excited.

V. CONCLUSIONS

The total spin-lattice relaxation rates $1/T_1$ were measured in GaAs, GaSb, and InAs from 4 to 300 K. These data, along with those of Bridges and Clark for InSb, are presented. The magnetic relaxation was separated from the quadrupolar relaxation for these crystals, except for GaSb. The quadrupolar relaxation is separated into two parts, relaxation by acoustic phonons, which predominates at lower temperatures, and relaxation by optical phonons, which becomes important at higher temperatures. The data were fitted by a four-parameter phenomenological model to within $\pm 5\%$ over the entire temperature range. The fit parameters are the amplitudes and characteristic frequencies of the acoustic- and optical-phonon processes (Table II).

The relative magnitudes of the relaxation by the acoustic and optical phonons can be understood qualitatively in terms of a dipole mechanism. No theories have been able to account for the amplitudes satisfactorily. We speculate that the work on the electric-field-gradient tensors for group-III-V compounds using nuclear acoustic resonance[22] may help to explain the observed magnitudes.

ACKNOWLEDGMENTS

We are grateful to F. Bridges and R. Orbach for illuminating discussions and helpful suggestions.

---

*Work supported in part by the AFOSR (Grant No. 68-1528) and the National Science Foundation (Grant No. GP29878).

†Present address: Loyola Marymount University, Los Angeles, Calif. 90045.

[1]F. Bridges and W. G. Clark, Phys. Rev. 164, 288 (1967).
[2]W. G. Clark, *Colloque Ampere XV* (North-Holland, Amsterdam, 1969).
[3]F. Bridges, Phys. Rev. 164, 299 (1967).
[4]J. A. McNeil, following paper, Phys. Rev. B 13, 4714 (1976).
[5]Cominco American, Inc., West 818 Riverside Ave., Spokane, Wash.
[6]Monsanto Co., 7210 Lafayette St., Santa Clara, Calif. 95052.
[7]W. G. Clark, Rev. Sci. Instrum. 35, 316 (1964).
[8]W. G. Clark and J. A. McNeil, Rev. Sci. Instrum. 44, 844 (1973); J. A. McNeil and W. G. Clark, First Specialized Colloque Ampere, Krakow, Poland, 1973 (unpublished).
[9]J. A. McNeil, Ph.D. thesis (University of California, Los Angeles, 1973) (unpublished).
[10]W. W. Warren and W. G. Clark, Phys. Rev. 177, 600 (1969).
[11]R. L. Mieher, Phys. Rev. 125, 1537 (1962); J. Zak, Physica (Utr.) 30, 401 (1964).
[12]G. H. Fuller and V. W. Cohen, Nucl. Data Tables A5, 433 (1969).
[13]J. Van Kranendonk and M. B. Walker, Can. J. Phys. 46, 2441 (1968).
[14]M. H. Cohen and F. Reif, in *Solid State Physics*, edited by F. Seitz and D. Turnbull (Academic, New York, 1957), Vol. 5.
[15]D. L. Price, J. M. Rowe, and R. M. Nicklow, Phys. Rev. B 3, 1268 (1971).
[16]J. L. T. Waugh and G. Dolling, Phys. Rev. 132, 2410 (1963).
[17]J. C. Phillips, Phys. Rev. 113, 147 (1959).
[18]S. S. Mitra, in *Optical Properties of Solids*, edited by S. Nudelman and S. S. Mitra (Plenum, New York, 1969).
[19]E. G. Wikner, W. E. Blumberg, and E. L. Hahn, Phys. Rev. 118, 631 (1960).
[20]S. K. Joshi, R. Gupta, and T. P. Das, Phys. Rev. 134, A693 (1964).
[21]M. Hass and B. W. Henvis, J. Phys. Chem. Solids 23, 1099 (1962).
[22]R. K. Sundfors, Phys. Rev. B 10, 4244 (1974).